

Large magnetoresistance in nonmagnetic π -conjugated semiconductor thin film devices

Ö. Mermer,¹ G. Veeraraghavan,² T. L. Francis,^{2,3} Y. Sheng,¹ D. T. Nguyen,¹ M. Wohlgenannt,^{1,*} A. Köhler,⁴ M. K. Al-Suti,⁵ and M. S. Khan⁵

¹*Department of Physics and Astronomy, The University of Iowa, Iowa City, Iowa 52242-1479, USA*

²*Department of Electrical and Computer Engineering, The University of Iowa, Iowa City, Iowa 52242-1595, USA*

³*OMR Sensors Inc., Dubuque, Iowa 52002, USA*

⁴*Institute of Physics, University of Potsdam, Am Neuen Palais 10, 14469 Potsdam, Germany*

⁵*Department of Chemistry, Sultan Qaboos University, P. O. Box 36, Al Khod 123, Sultanate of Oman*

(Received 3 May 2005; revised manuscript received 18 August 2005; published 10 November 2005)

Following the recent observation of large magnetoresistance at room temperature in polyfluorene sandwich devices, we have performed a comprehensive magnetoresistance study on a set of organic semiconductor sandwich devices made from different π -conjugated polymers and small molecules. The study includes a range of materials that show greatly different chemical structure, mobility, and spin-orbit coupling strength. We study both hole and electron transporters at temperatures ranging from 10 K to 300 K. We observe large negative or positive magnetoresistance (up to 10% at 300 K and 10 mT) depending on material and device operating conditions. We discuss our results in the framework of known magnetoresistance mechanisms and find that none of the existing models can explain our results.

DOI: [10.1103/PhysRevB.72.205202](https://doi.org/10.1103/PhysRevB.72.205202)

PACS number(s): 73.50.Jt

I. INTRODUCTION

Organic π -conjugated materials have been used to manufacture devices such as organic light-emitting diodes,^{1,2} photovoltaic cells,^{3–5} and field-effect transistors.^{6–8} Recently there has been a growing interest in spin^{9–11} and magnetic field effects^{12–19} in these materials. Kalinowski and coworkers demonstrated that the electroluminescence in devices made from the small molecule tris-(8-hydroxyquinoline) aluminium (Alq₃)¹⁵ and an electrophosphorescent compound¹⁶ can be modulated by weak magnetic fields. They explained their findings assuming that the magnetic field affects the balance between luminescent singlet excitons and nonluminescent triplet excitons. In addition, a relatively small effect of the magnetic field on the current was also observed¹⁵ that was explained by singlet exciton dissociation at the cathode. Davis and Bussmann extended the magnetic field range studied to several teslas,¹⁷ and demonstrated an effect of the magnetic field on the electroluminescence and suggested spin-dependent triplet-triplet annihilation as the origin. In their more recent work, they, however, concluded that triplet-triplet annihilation cannot be responsible for the effect at low magnetic fields because the effect is especially large under low bias where the triplet density is very small.²⁰ During the study of sandwich devices made from the π -conjugated polymer polyfluorene, we recently observed¹² a large and intriguing magnetoresistive effect, which we dubbed organic magnetoresistance (OMAR). OMAR may find application in magnetic field sensors, e.g., in organic light-emitting diode interactive displays (patent pending, see demonstration video in Ref. 12).

II. EXPERIMENTAL

Here we describe the sources for the various organic semiconductors that we used in our study. The π -conjugated

polymer polyfluorene was purchased from American Dye Source, Inc., whereas regio-regular Poly(3-hexylthiophene-2,5-diyl) (RR-P3HT) and regio-random Poly(3-octylthiophene-2,5-diyl) (RRA-P3OT) were purchased from Sigma Aldrich. The π -conjugated small molecule Alq₃ was purchased from H. W. Sands Corporation and pentacene was purchased from Sigma Aldrich. The 5,8-diethynyl-2,3-diphenylquinoxaline unit and its platinum-containing polymer (Pt-PPE) were prepared according to published procedures.^{21,22} The organic polymer (PPE) was synthesized by palladium-catalyzed polycondensation of 1,4-bis(n-octyloxy)-2,5-diiodobenzene and 5,8-diethynyl-2,3-diphenylquinoxaline in a 1:1 ratio.

The fabrication of the organic sandwich devices started with glass substrates coated with 40 nm of indium-tin-oxide (ITO) purchased from Delta Technologies. The conducting polymer Poly(3,4-ethylenedioxythiophene)-poly(styrenesulfonate) (PEDOT), purchased from H. C. Starck was spin coated at 2000 revolutions per minute (rpm) on top of the ITO in some devices to provide an efficient hole injecting electrode. All other manufacturing steps were carried out in a nitrogen glovebox. The active polymer film was spin coated onto the substrate from a chloroform solution. The semiconductor film thickness was varied by using different concentrations of polymer solution (5–30 mg/ml). The small molecular film layers were made by thermal evaporation. A Ca cathode followed by a capping layer of Al were then deposited by thermal and electron beam evaporation, respectively, at a base pressure of $\approx 1 \times 10^{-6}$ mbar on top of the organic thin films. The device area was $\approx 1 \text{ mm}^2$ for all devices except for the ITO/polyfluorene/Ca device, where the device area was $\approx 10 \text{ mm}^2$. The general device structure used for our measurements was metal/organic semiconductor/metal (see Fig. 1). We studied both soxhlet purified RR-P3HT and as received RR-P3HT. The initial soxhlet purification step was performed for 8–12 h using hexane to remove low mo-

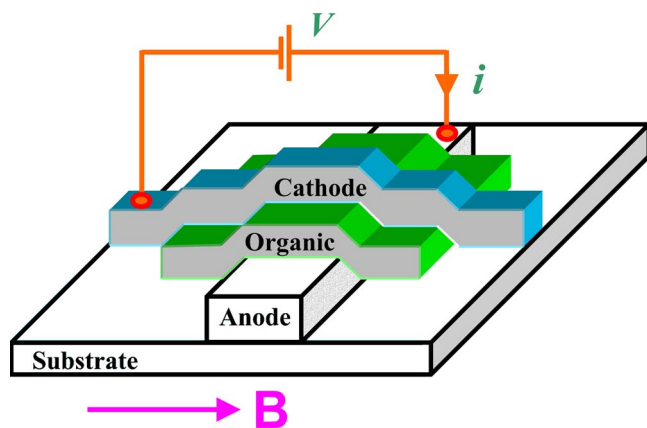


FIG. 1. (Color online) A schematic drawing of the device and the magnetoresistance experiment.

lecular weight components. The second step was performed for 24 h using methanol to remove metallic impurities. The third step was performed for 8–12 h using chloroform to dissolve the pure polymer. A roto-vap was used to separate the polymer from the solution.

A schematic drawing of the device and the experiment are shown in Fig. 1. The samples were mounted on the cold finger of a closed-cycle helium cryostat located between the poles of an electromagnet. The magnetoresistance ratio, $\Delta R/R$, was determined by measuring the current at a constant applied voltage for different magnetic fields, B . The electroluminescence of the devices was measured with a photomultiplier tube that was shielded from the magnetic field using high-saturation mu-shield foil.

III. EXPERIMENTAL RESULTS

A. Organic Magnetoresistance in polymer devices

1. Polyfluorene devices

We initially observed OMAR in polyfluorene sandwich devices.¹² These results are described in detail in our earlier publication,¹² here we show only the room temperature data in Fig. 2 for different applied voltages. We summarize the findings of our previous work: (1) The effect is unexpectedly large for nonmagnetic devices, up to $\Delta R/R=10\%$ at $B=10$ mT at room temperature. (2) The OMAR curves are independent of the angle between film plane and the applied magnetic field. (3) The measured OMAR effect does not critically depend on the choice of the top electrode (cathode) materials. This implies that the magnetic field acts on the hole current since it occurs also in hole-only devices, namely those with Au cathodes where only very weak electroluminescence is observed. In particular, this shows that OMAR is not related to excitonic processes, such as the ones that have previously been invoked to explain the magnetic field effect on the electroluminescence.^{15,18} We note that holes are the majority carriers in polyfluorene, since the hole mobility is orders of magnitude larger than that for the electrons.²³

Next, we examined whether the magnetic field acts on (i) hole injection at the anode or on (ii) hole transport through

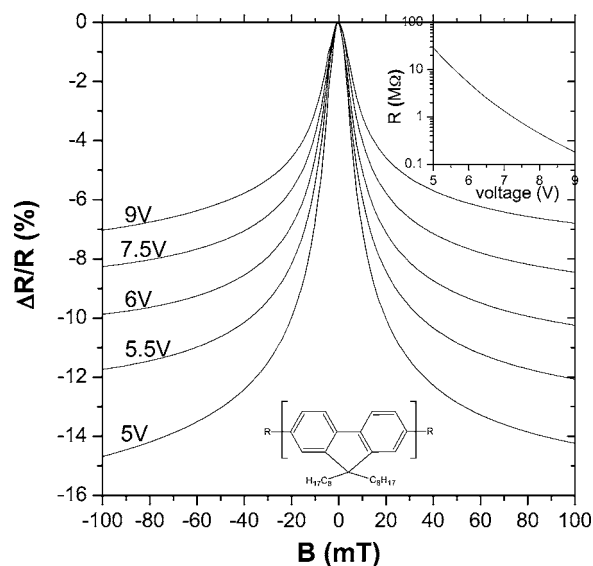


FIG. 2. Magnetoresistance, $\Delta R/R$ curves, measured at room temperature in an ITO/PEDOT/polyfluorene(≈ 100 nm)/Ca device at different voltages. The inset shows the device resistance as a function of the applied voltage.

the polyfluorene layer. In general, we can expect that if OMAR is of type (i), then it should be strongest in injection-limited devices; whereas if OMAR is of type (ii), then it should be strongest in bulk-limited devices. The current tends to be injection-limited if the (here anode) metal work function is mismatched relative to the semiconductor (here valence) band.²⁴ Injection-limited devices are characterized by much larger onset voltages compared to those observed in bulk-limited devices, because a considerable fraction of the voltage will drop at the interface. We found that OMAR in polyfluorene strongly depends on the choice of anode material. In particular, using PEDOT as the anode results in a significant reduction in the onset voltage and an increase in the observed OMAR effect. The reduced onset voltage and increased magnetoresistance can be rationalized considering the decrease in the hole-injection barrier and the resulting reduction of the interface resistance. The observation that OMAR is largest in the device with the smallest interface resistance implies that it is a bulk effect.

As a further test to distinguish between (i) and (ii), we fabricated devices with different polymer film thickness. If OMAR were of type (i), then we would expect it to be largest in a device with a thin organic layer, since the interface resistance would make up a larger fraction of the total device resistance. We, however, found that the observed OMAR magnitude was similar at comparable currents in all devices independent of polyfluorene film thickness. We confirmed that the OMAR effect is not related to (unintentional and/or intentional) impurities, such as the leftover catalysts from the polymerization reaction.

Figure 3 shows the I - V characteristics of a PEDOT/polyfluorene/Ca device with and without the applied magnetic field, $B=100$ mT. It is seen that the I - V curve with the applied magnetic field is approximately reproduced when the I - V curve without the magnetic field is translated by a constant voltage shift. As a matter of fact, Fig. 3, inset

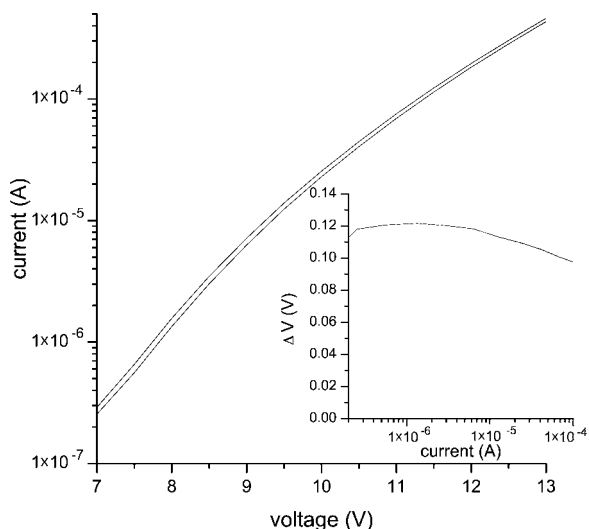


FIG. 3. Current voltage characteristics with (upper curve) and without (lower curve) applied magnetic field, $B=100$ mT, in a PEDOT/polyfluorene(≈ 150 nm)/Ca device. The inset shows that the change in voltage ΔV caused by the magnetic field at constant current is largely independent of the driving current.

shows that the voltage shift, ΔV caused by B at constant current is quite insensitive to the driving current, at least in the current range studied in Fig. 3. This peculiar behavior may hold clues regarding the origin of OMAR and may serve as a benchmark for future theories. We note that for a classical magnetoresistor—where a B field of a given strength induces a fractional change in resistance, $\Delta R/R$ of a well-defined, corresponding magnitude—we would expect $\Delta V/V$ and not ΔV to be approximately independent of the driving current. Therefore, we would expect ΔV to increase with increasing voltage, whereas ΔV even slightly decreases in Fig. 3. As a counterexample, however, we would like to mention weak localization where the change in conductivity, $\Delta\sigma$ rather than the fractional change, $\Delta\sigma/\sigma$ is directly related to the magnetic field. In Sec. III B, the section on OMAR in Alq_3 devices, we will present a more extensive analysis of the voltage effect.

Figure 4 shows OMAR curves in an ITO/polyfluorene (≈ 60 nm)/Ca device. We found that the ITO-polyfluorene interface is less suitable for hole injection than the PEDOT-polyfluorene interface; resulting in a large increase in turn-on voltage of the device and a reduction in the magnitude of OMAR. Therefore, the measurements were performed at 200 K to reduce thermal drift. Importantly, we also observed positive magnetoresistance¹⁴ in the ITO anode device at high applied voltages and large current densities. We have not yet completed a careful study of the crossover behavior in polyfluorene devices, partly because irreversible changes often occurred to the devices at the large current densities usually needed for crossover. Nevertheless, this shows that OMAR may be either negative or positive, and that a potential theoretical explanation of OMAR will, therefore, have to allow for positive and negative magnetoresistance. A more thorough discussion of the crossover behavior will be presented in polythiophene devices in Sec. III A 3. This observation also implies that the approximate constancy of the voltage

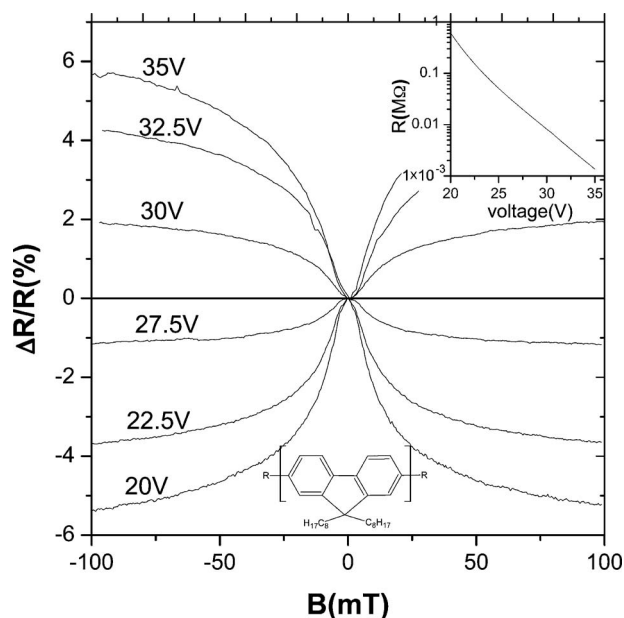


FIG. 4. Magnetoresistance, $\Delta R/R$ curves, measured at 200 K in an ITO/polyfluorene(≈ 60 nm)/Ca device at different voltages. The inset shows the device resistance as a function of the applied voltage.

shift, ΔV observed in Fig. 3 for a PEDOT/polyfluorene/Ca device cannot hold true in the entire “parameter space” of polyfluorene OMAR devices: ΔV must obviously change sign as OMAR changes sign. As a matter of fact, Fig. 3 shows that ΔV (slightly) decreases with increasing current, possibly anticipating a change of sign. However, an extrapolation of the data for ΔV in Fig. 3 indicates that the change in sign lies outside the achievable current-voltage range in PEDOT anode devices. As we will show in Sec. III B, ΔV is also approximately independent of the driving current in PEDOT/ Alq_3 /Ca devices. Therefore, the constancy of ΔV is an important observation, although its validity is certainly limited to a finite part of the parameter space of OMAR, and it is not valid close to the transition region between positive and negative OMAR.

2. Magnetic field effect on electroluminescence

OMAR devices have the unique property of showing large magnetoresistance while being also highly electroluminescent. Figure 5 shows the magnetic field effect on the electroluminescence in a PEDOT/polyfluorene/Ca device measured at a constant voltage or at a constant current. These data show that the magnetic field effect exists both in the electric and luminescent measurements. Note that the shapes of the magnetic field effect on the current and that of the magnetic field effect on the electroluminescence are equivalent and that they, therefore, share a common origin. The magnetic field effect on the electroluminescence is greatly reduced when measuring at a constant current rather than a constant applied voltage. To rationalize these observations, we note that the electroluminescence intensity, EL , may be written as

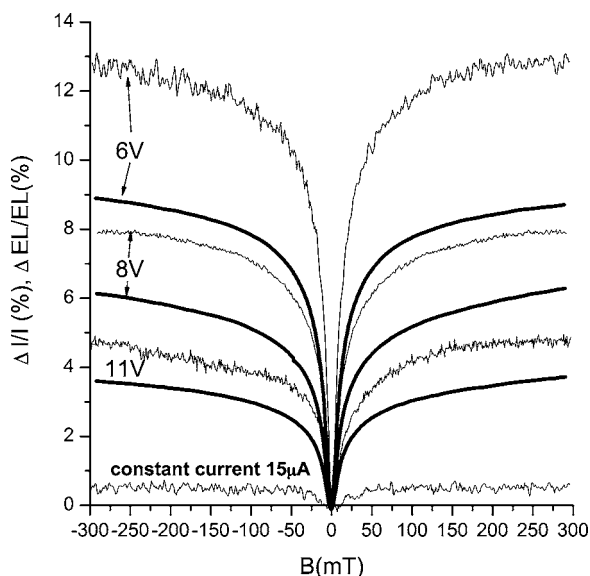


FIG. 5. Magnetic field effect on current (bold) and electroluminescence in a PEDOT/polyfluorene (≈ 100 nm)/Ca device measured at several different constant voltages. The magnetic field effect on electroluminescence measured at a constant current, $15 \mu\text{A}$ corresponding to ≈ 8 V is also shown.

$$EL \propto \eta I, \quad (1)$$

where η is the electroluminescence quantum efficiency and I is the current. There are two distinct possibilities for a magnetic field effect on electroluminescence: (i) $I=I(B)$ and (ii) $\eta=\eta(B)$. We note that all other works on magnetic field effects in organics,^{15–18} that we know of, assumed that the magnetic field affects the emission efficiency directly [type (ii)], whereas the magnetoresistance effect was largely overlooked. It is relatively straightforward to distinguish between the two possibilities: an effect of type (i) will show up in both electrical [since $I=I(B)$] and luminescent measurements [since $EL=EL(I)$] with comparable strength; whereas an effect of type (ii) will show up strongly only in the luminescent measurement, since the current should not depend much on η . Moreover, for an effect of type (ii), it should be largely irrelevant whether the measurement is performed at a constant voltage or at a constant current. From the data shown in Fig. 5, therefore, it follows that the magnetic field effect observed here is of type (i). We note that a high-field effect at fields greater than several hundred mT was previously studied by Davis and Bussmann²⁵ and meets the criteria of a type (ii) effect. In the remainder of the manuscript, we will be concerned exclusively with the type (i), low-field ($B < 100$ mT) effect.

3. Regio-Regular and regio-random polythiophene devices

Next we extend our study to include RR-P3HT and RRa-P3OT. In contrast to polyfluorene, RR-P3HT and RRa-P3OT do not contain benzene rings. Since it is known that the conjugated rings in graphene lead to unusual magnetic properties,²⁶ one might speculate that OMAR is similarly caused by the benzene ring. In the following, however, we

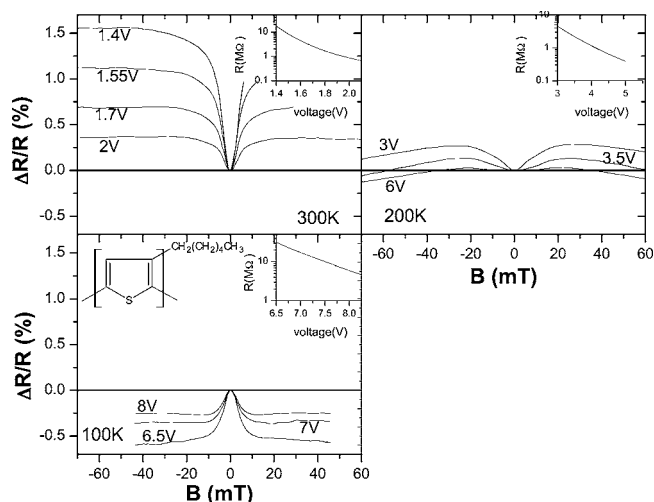


FIG. 6. Magnetoresistance, $\Delta R/R$ curves, in an ITO/PEDOT/RR-P3HT (≈ 100 nm)/Ca device measured at different temperatures (100 K, 200 K, and 300 K). The insets show the device resistance as a function of the applied voltage.

will show that this is not the case. RR-P3HT was also selected due to its high mobility among polymers and its well-known usage in transistors, smart pixels, and optoelectronic devices.^{27–29} It is reasonable to expect that larger mobility may lead to an increase in OMAR response, since, e.g., classical magnetoresistance is proportional to the second power of the mobility. The reason for the high carrier mobilities in transistors is the self-organization of RR-P3HT chains resulting in a lamellae structure.^{28,30} Delocalization of the charge carriers among the lamellae has been invoked to be the reason for the high interlayer mobility, with values reported as high as $0.1 \text{ cm}^2 \text{ V}^{-1} \text{ s}^{-1}$.²⁸ RRa-P3OT, which has a similar chemical structure as RR-P3HT, has a lamellae structure to a lesser degree because of its regio-random substitution and the carrier mobility is consequently much smaller, around $10^{-4} \text{ cm}^2 \text{ V}^{-1} \text{ s}^{-1}$.^{28,30,31}

Figure 6 shows measured OMAR traces as a function of temperature in an ITO/PEDOT/RR-P3HT/Ca device. The magnitude of the observed OMAR effect is small (less than 1.5%). The data shows that the OMAR effect can be both positive and negative in RR-P3HT, mostly dependent on temperature. At room temperature, the OMAR effect is completely positive, whereas at 100 K, the effect is negative. At 200 K, a transition from positive to negative magnetoresistance occurs as the voltage increases in RR-P3HT. A similar transition occurs in polyfluorene when the voltage is decreased.¹⁴ This intriguing behavior may hold a clue for identifying the mechanism responsible for the magnetoresistance effect. We studied both soxhlet purified RR-P3HT and as received RR-P3HT. We did not find any significant difference between the two samples. This supports our conclusion from the experiments in polyfluorene devices that OMAR is not caused by impurities.

We observed only negative OMAR traces in ITO/PEDOT/RRa-P3OT/Ca devices, shown in Fig. 7, at all temperatures spanning the range between 10 K and 300 K. The data measured in RRa-P3OT is noisier than in RR-P3HT, presumably because of the increased disorder and

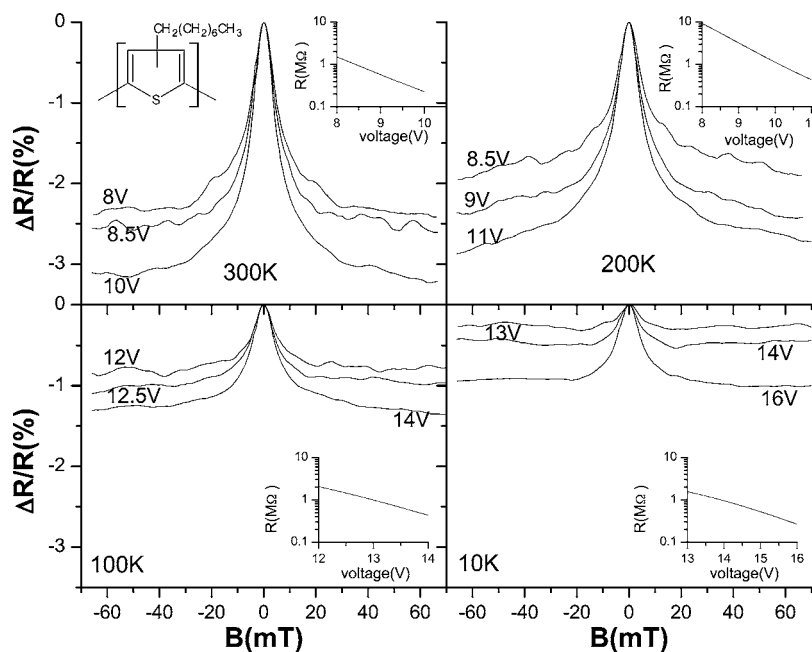


FIG. 7. Magnetoresistance, $\Delta R/R$ curves, in an ITO/PEDOT/RRa-P3OT (≈ 100 nm)/Ca device measured at different temperatures (10 K, 100 K, 200 K, and 300 K). The insets show the device resistance as a function of the applied voltage.

possibly lower purity of the RRa-P3OT polymer. The magnitude of the measured OMAR effect in RRa-P3OT devices was found to be consistently higher than that of the RR-P3HT devices. This shows that low disorder and/or high mobility is not a necessary prerequisite for large OMAR response.

4. Polyphenylene ethynylene (PPE) and platinum-containing PPE: the influence of spin-orbit coupling

We studied OMAR in two π -conjugated polymers containing triple bonds, namely (i) the platinum-containing polymer (Pt-PPE) shown in Fig. 8 and (ii) a very similar polymer without platinum shown in Fig. 9. It was shown previously that the platinum atom does not interrupt the

conjugation.^{32,33} We studied these polymers to examine a possible interdependence between spin-orbit coupling and the OMAR effect. The heavy platinum atom introduces relatively strong spin-orbit coupling³¹ and the spin orientation ceases to be a good quantum number. In an attempt to quantify the strong spin-orbit coupling introduced by the platinum atom, we measured the photoluminescence spectra (Fig. 10) of these two polymers. In Pt-PPE, both fluorescence (singlet exciton emission) and phosphorescence (triplet exciton emission) bands^{32,33} are observed; whereas, in the polymer without platinum, the phosphorescence is absent.³⁴

It is well known that the observation of triplets requires intersystem crossing from the singlet to the triplet manifold. The fact that phosphorescence is observed together with fluorescence implies that the intersystem crossing time, τ_{ISC}

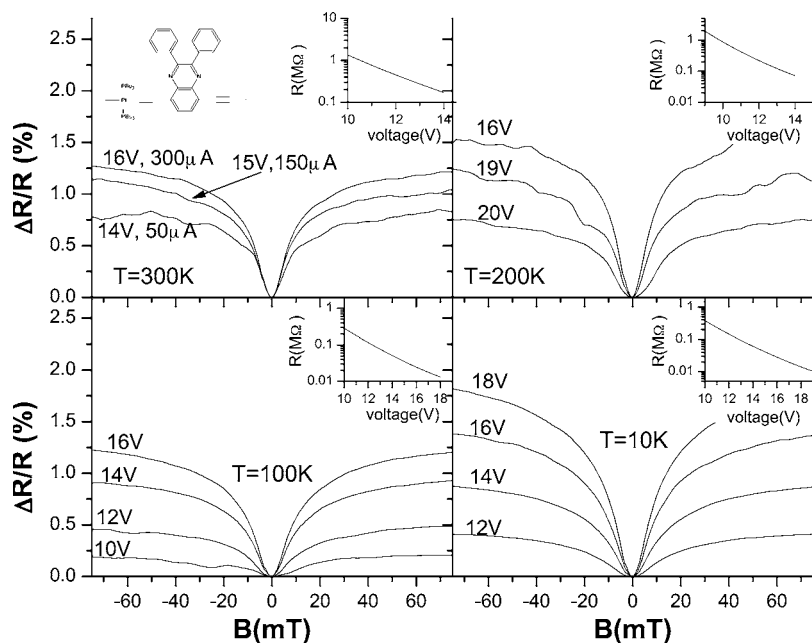


FIG. 8. Magnetoresistance, $\Delta R/R$ curves, in an ITO/PEDOT/Pt-PPE/Ca device measured at different temperatures (10 K, 100 K, 200 K, and 300 K). The measurements were performed at the constant voltages specified, the approximate current levels are also indicated for the corresponding room temperature data. The insets show the device resistance as a function of the applied voltage.

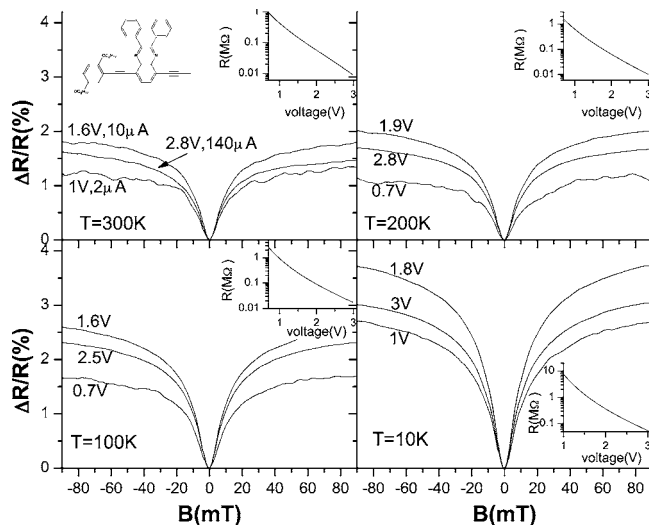


FIG. 9. Magnetoresistance, $\Delta R/R$ curves, in an ITO/PEDOT/PPE/Ca device measured at different temperatures (10 K, 100 K, 200 K, and 300 K). The measurements were performed at the constant voltages specified, the approximate current levels are also indicated for the corresponding room temperature data. The insets show the device resistance as a function of the applied voltage.

must be of a comparable magnitude as the singlet exciton lifetime, which is known to be typically around 300 ps.³⁵ Wilson *et al.*³² note that although the spin-orbit coupling induced by the heavy platinum atom has been shown to produce close to 100% intersystem crossing,³⁶ there is still more singlet emission observed in photoluminescence, because, despite the phosphorescence transition being partially allowed, the radiative decay rates from the triplet states are still only of the order of 10^3 s^{-1} in comparison with nonradiative decay rates of 10^6 – 10^5 s^{-1} , so only 1 in 1000 of the

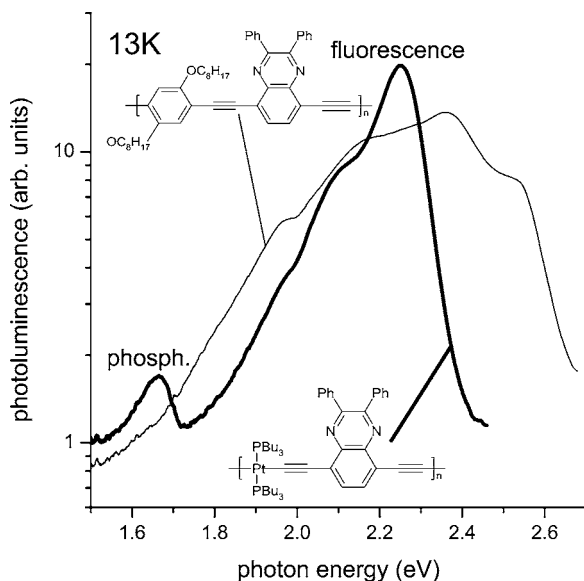


FIG. 10. The photoluminescence of PPE (solid line) and Pt-PPE (bold line) at 13 K. The emission bands of Pt-PPE due to fluorescence and phosphorescence are assigned.

triplets generated emits light.³⁷ This then allows the conclusion that $\tau_{ISC} \ll 1 \text{ ns}$; whereas, a typical value for organic polymers is $\tau_{ISC} \approx 10 \text{ ns}$.³⁵ We have recently studied the same two polymers using an electron spin resonance technique.³³ We found that the spin-relaxation times of the spin-1/2 electrons and holes in the organic polymer are very long, exceeding 1 ms (see also Ref. 38) at liquid Helium temperatures, whereas fast spin-relaxation (compared to the time scale of microwave-induced spin-flips) occurs for the platinum-containing polymer.

Figures 8 and 9 show OMAR traces measured in ITO/PEDOT/Pt-PPE/Ca and ITO/PEDOT/PPE/Ca devices, respectively, measured at different temperatures. It is seen that the OMAR effect is positive and of similar magnitude within the current range studied (the measurements were performed at the constant voltages specified in Figs. 8 and 9, the approximate current levels are also indicated for the corresponding room temperature data) at all temperatures for both polymers. Similar to the trend we previously observed in positive OMAR traces in polyfluorene,¹⁴ the following trend regarding the magnitude of the positive OMAR effect was observed in Fig. 9: Initially the OMAR magnitude increases with increasing voltage, reaches a maximum, and then decreases with increasing voltage. We believe that this is the general trend for positive OMAR, but this conclusion is somewhat speculative, however, since the entire necessary voltage parameter space was not accessible in all devices at all temperatures. Another important observation is that the width of the OMAR cones remains unaffected by the platinum atom. Altogether, we therefore obtain the result that spin-orbit coupling has apparently little effect on OMAR (at least qualitatively). This in turn suggests that OMAR is not related to spin but is likely related to an orbital effect. Strictly speaking, based on the analysis presented above, fast spin-dependent processes occurring at time scales $\ll 1 \text{ ns}$ are still a possibility. In particular, our data show that mechanisms involving intersystem crossing in excitons^{15,18} cannot explain OMAR (see also Sec. IV).³⁹

B. Organic magnetoresistance in small molecule devices

Having demonstrated OMAR in polymers, it is natural to ask whether OMAR also exists in small molecules, e.g., the prototypical small molecule Alq_3 . Indeed, we have recently shown that large OMAR can also be achieved in Alq_3 .¹³ This extension is highly relevant both from an application as well as a scientific point of view. Whereas polymers are quasi-one-dimensional, Alq_3 corresponds more to quasi-zero-dimensional. Whereas polyfluorene and most other π -conjugated polymers are hole transporters, meaning that the hole mobility greatly exceeds that for electrons,²³ Alq_3 is an electron transporter.⁴⁰

A detailed study of the OMAR effect in Alq_3 devices can be found in our earlier publication.¹³ Here only the room temperature data is shown in Fig. 11. After a summary of our previous results in Alq_3 , we will extend our study in small molecules to include pentacene. (1) As in polyfluorene, the effect is independent of the sign and direction of the magnetic field, and shows only a weak temperature dependence.

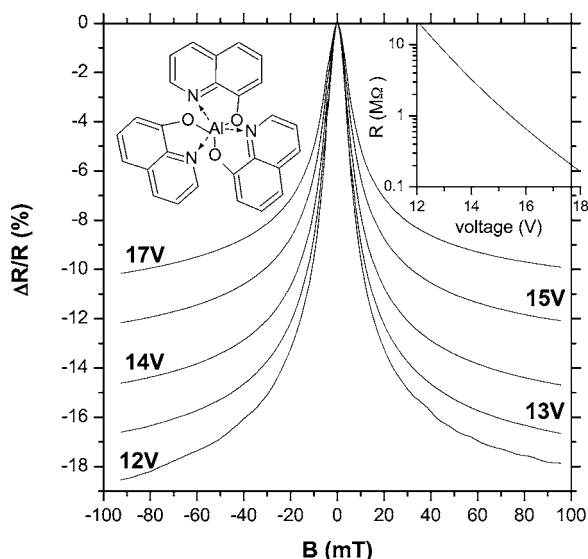


FIG. 11. Magnetoresistance, $\Delta R/R$ curves, measured at room temperature in an ITO(30 nm)/PEDOT(≈ 100 nm)/Alq₃(≈ 100 nm)/Ca (≈ 50 nm including capping layer) device at different voltages. The inset shows the device resistance as a function of the applied voltage.

(2) In distinction to our results in polymers, we found that both I - V and OMAR responses critically depend on the choice of electron-injecting cathode material. Ca cathodes result in low onset voltage and large OMAR response; whereas, using Al results in a drastic increase in onset voltage and decrease in OMAR magnitude. The situation is even more drastic when using a Au cathode. The increased onset voltage and decreased OMAR can be rationalized considering the increase in the electron-injection barrier and the resulting increase in interface resistance, respectively, when using high work function cathodes (Ca has the lowest work function, followed by Al, whereas Au has one of the largest work functions). This strong dependence of OMAR on the choice of cathode material was to be expected since Alq₃ is an electron transporter.⁴⁰ (3) Compared to bulk-limited devices, injection-limited devices show higher onset voltages because a large fraction of the applied voltage drops at the contact interface. Therefore, Ca cathode devices are the least injection-limited devices, but show the largest OMAR response. Since carrier injection does not contribute to the resistance (and therefore, not to the magnetoresistance) in bulk-limited devices,²⁴ this shows that OMAR is a magnetotransport effect and not an effect on carrier injection. (4) Studying the I - V characteristic of the Ca cathode device, we found that it obeys a power law typical of space-charge limited current⁴¹ and that the device is, therefore, bulk limited. This confirms our conclusion that OMAR is a magnetotransport effect. We found that the experimental data are consistent with the notion that the magnetic field affects the prefactor in the power law, rather than its exponent. We note that the exponent is directly related to the typical trap energy, whereas the prefactor is proportional to the mobility.¹³ (5) In Ref. 13, we also examined the magnetic field effect on the electroluminescence and electroluminescence efficiency. Our results, which are very similar to the ones presented in the

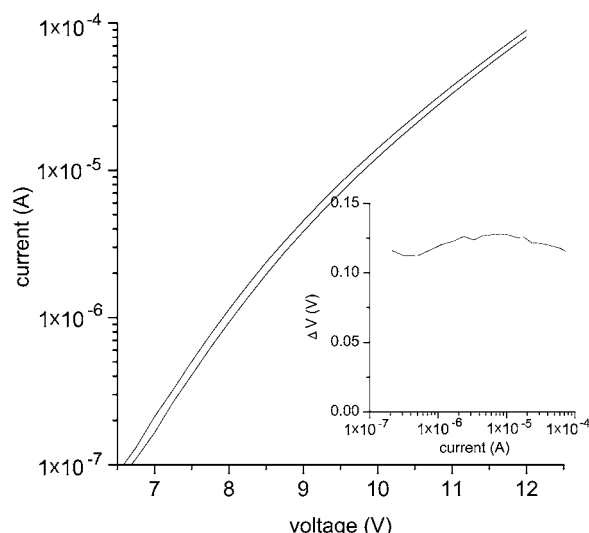


FIG. 12. Current voltage characteristics with (upper curve) and without (lower curve) applied magnetic field, $B=100$ mT, in a PEDOT/Alq₃ (≈ 100 nm)/Ca device. The inset shows that the change in voltage ΔV caused by the magnetic field at constant current is largely independent of the driving current.

present paper for polyfluorene, showed that the low-field effect on the electroluminescence is a consequence of the magnetoresistance effect.

Figure 12 shows the I - V characteristics of a PEDOT/Alq₃/Ca device with and without the applied magnetic field, $B=100$ mT. Similar to our results in polyfluorene, the Fig. 12 inset shows that ΔV caused by B at constant

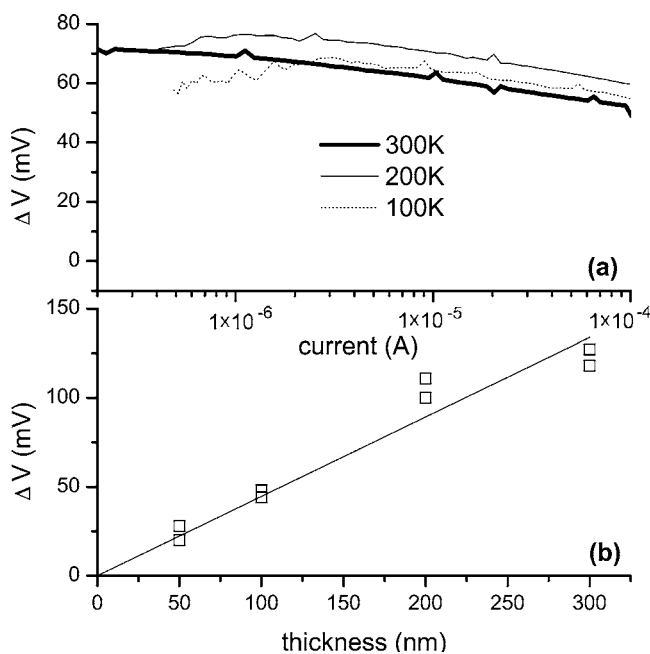


FIG. 13. (a) Magnitude of the magnetic field effect on voltage ΔV in applied magnetic field, $B=10$ mT as a function of the biasing current in a PEDOT/Alq₃ (100 nm)/Ca device at three different temperatures. (b) ΔV at 10 mT and 300 K at a biasing current of 100 μ A in a series of devices as a function of the Alq₃ layer thickness. The solid line is a linear fit.

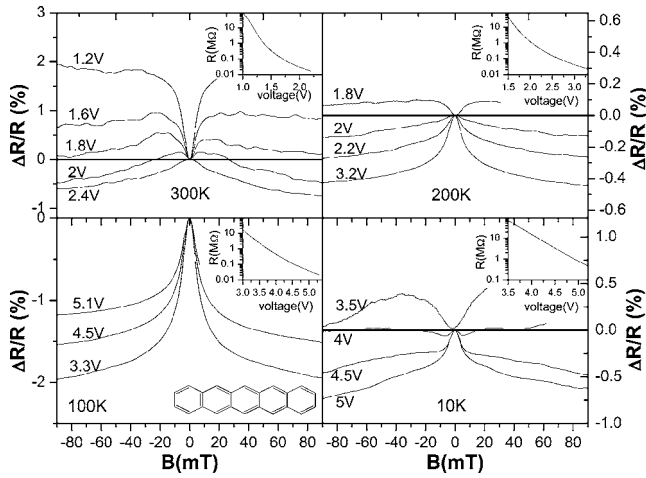


FIG. 14. Magnetoresistance, $\Delta R/R$ curves, in an ITO/PEDOT/pentacene(≈ 100 nm)/Ca device measured at different temperatures (10 K, 100 K, 200 K, and 300 K). The insets show the device resistance as a function of the applied voltage.

current is largely independent of the driving current also in Alq_3 . Figure 13(a) shows similar data in another PEDOT/ Alq_3 /Ca device for $B=10$ mT at three different temperatures, namely 300 K, 200 K, and 100 K. We find that ΔV is also relatively insensitive to changes in temperature. These observations suggest that the voltage effect, rather than the effect on current or resistance, may be the more fundamental one. Furthermore, we find that $\Delta V \propto d$, where d is the organic layer thickness [see Fig. 13(b)]. Therefore, we obtain the potentially important result that $\Delta E = \Delta V/d$ in PEDOT/ Alq_3 /Ca devices is a strong function only of B . As is known from the theory of relativity, an applied B field may be perceived as a change in the electrical field ΔE if the electron moves at velocity, $v = \Delta E/B \approx 10^8$ m/s, where we used the values $\Delta E = 0.1\text{V}/100$ nm and $B = 10$ mT. To the best of our knowledge, such large velocities do not occur in organic light-emitting diodes; therefore, another explanation for the approximate constancy of ΔE must be found. The fact that $\Delta V \propto d$ is further proof for the notion that OMAR is a bulk effect. If it were an interface effect, ΔV should be constant or even decrease as d increases.

Figure 14 shows the temperature dependence of OMAR in an ITO/PEDOT/pentacene/Ca device. OMAR in the pentacene device is much smaller compared to the Alq_3 device. The picture of OMAR in pentacene is relatively complex. We found that OMAR can be positive or negative at 10 K, 200 K, and 300 K. At these temperatures, the transition from positive to negative magnetoresistance occurs as the bias voltage increases. OMAR at 100 K, however, follows a different trend. The effect was negative at all biases studied, with the smallest bias giving the largest negative effect.

IV. DISCUSSION

A. Universality of the OMAR effect

Figure 15 shows the normalized magnetoresistance ratio, $\Delta R/R$, traces of all the tested devices at room temperature.

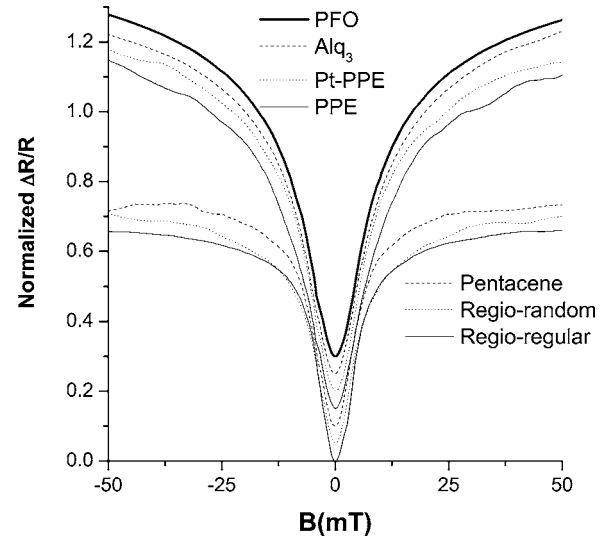


FIG. 15. Normalized magnetoresistance ratio, $\Delta R/R$ curves, of PEDOT/organic semiconductor/Ca devices using different organic semiconductors measured at room temperature. The data has been offset for clarity.

The normalization was done with respect to the magnitude of the OMAR effect at 50 mT. It is seen from the figure that there are two groups of OMAR traces in organic semiconductor materials. One (pentacene, RR-P3HT, and RRA-P3OT) where the OMAR effect has saturated at 50 mT, and the other (polyfluorene, Alq_3 , Pt-PPE, and PPE) where the effect does not fully saturate. In the following, we will refer to the former traces as “fully saturated” and to the latter as “weakly saturated.” The functional dependence of the OMAR effect was found to be very similar in devices within a group. This is very surprising, since the chemical structures of these materials are quite different. The “universality” of the OMAR effect, therefore, suggests that the explanation for the origin of OMAR may be quite general and simple. Furthermore, the universality may point to the involvement of nuclear spin since the *local* chemical environment is very similar in all the materials studied. Future experiments in deuterated organic semiconductors may test this suggestion.

B. Empirical law for OMAR

We now aim to explore the functional dependence of OMAR on B , i.e., $(\Delta I/I)(B)$ (we found that the dependence $(\Delta V/V)(B)$ is identical to $(\Delta I/I)(B)$ in the PEDOT/polyfluorene/Ca and PEDOT/ Alq_3 /Ca devices and presumably also in the other devices). For this purpose, we plot a typical room temperature OMAR trace in a PEDOT/polyfluorene/Ca device (squares) and a PEDOT/RR-P3 HT/Ca device (circles) as representatives for the weakly saturated and fully saturated traces, respectively, on a log-log scale in Fig. 16. We note that as long as one stays away from the transition region where a crossover from negative to positive OMAR occurs, the functional form of the traces is independent of the particular choice of bias voltage. The solid curve through the polyfluorene data is a fit using an empirical law of the form $\Delta I/I = (\Delta I/I)_{\text{max}} [B/B$

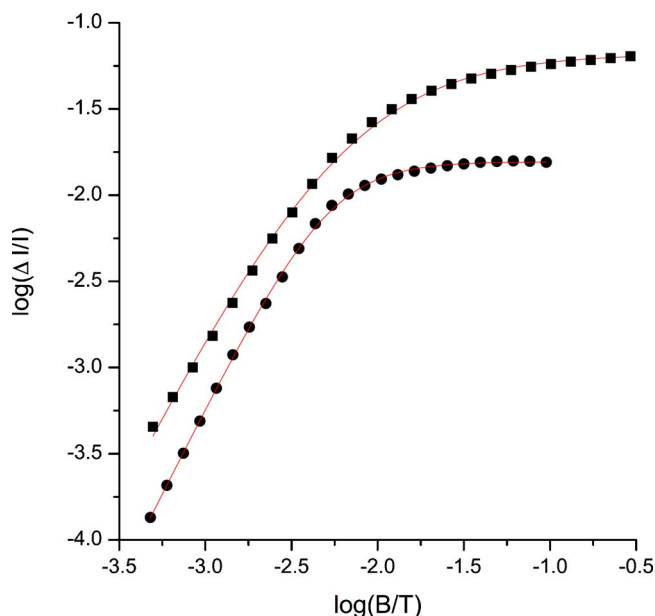


FIG. 16. (Color online) Room temperature OMAR traces in a PEDOT/polyfluorene/Ca device (squares) and a PEDOT/RR-P3HT/Ca device (circles) plotted on a log-log scale. The solid curves are fits using an empirical law of the form $\Delta I/I = (\Delta I/I)_{\max} [B/(B+B_0)]^2$ and $\Delta I/I = (\Delta I/I)_{\max} [B^2/(B^2+B_0^2)]$, respectively.

$+B_0]^2$, where $(\Delta I/I)_{\max}$ denotes the fractional change in current extrapolated to infinite field, and B_0 denotes the quarter-saturation field. This form was chosen since it reproduces the main features of the OMAR traces, namely $\Delta I/I \propto B^2$ at low B and the tendency toward saturation at large B . The fit is rather good over almost three orders of magnitude in B , where the value $B_0 = 5.89$ mT results in the best fit. However, we currently do not know whether this good agreement between the data and the empirical fit formula is coincidental. We found that the fit function used for polyfluorene fits all the traces for materials with weakly saturated behavior shown in Fig. 15 with the approximately same B_0 value, but does not fit RR-P3HT well, or any other material that shows fully saturated behavior. However, a fit using the function $\Delta I/I = (\Delta I/I)_{\max} [B^2/(B^2+B_0^2)]$ gives very accurate agreement (Fig. 16), where B_0 now is the half-saturation field. The value $B_0 = 5.15$ mT results in the best fit. Incidentally, a law of the form $\Delta I/I = (\Delta I/I)_{\max} [B^2/(B^2+B_0^2)]$ is what is predicted by simple theories of classical magnetoresistance.⁴² This suggests that the good fit is more than coincidental and that the fully saturated behavior is the more fundamental one. In the theory of classical magnetoresistance $B_0 \approx 1/\mu$ holds, where μ is the mobility. From our fitting results, we obtain $\mu \approx 10^6$ cm²/V s, clearly a nonsense result. This implies that although the functional form of classical magnetoresistance applies, the physics of OMAR is entirely different. Finally, we note that these two fitting functions can fit all the data we have observed at all temperatures, as long as one stays away from the transition region between negative and positive OMAR. Such transition region traces are most clearly seen in Fig. 6 at 200 K and Fig. 14 at 300 K. We have previously shown¹⁴ that the transition region curves can be

fitted well using the theory of weak localization and antilocalization. As we will show in Sec. IV C, however, it is doubtful that the weak-localization theory should apply to OMAR; therefore, we do not further discuss these fits here. We have been unable to find simple generalized fit functions that would allow fitting the transition region in a consistent manner.

C. Discussion of possible mechanisms

We now discuss candidate mechanisms for theories of OMAR. To the best of our knowledge, the mechanism causing OMAR is currently not known. Most magnetoresistance mechanisms rely on the presence of ferromagnetic materials and, therefore, are not applicable to our devices. We are familiar with the following mechanisms that cause magnetoresistance in nonmagnetic materials: (1) classical magnetoresistance, (2) hopping magnetoresistance,⁴³ (3) electron-electron (e-e) interaction,⁴⁴ and (4) weak localization.⁴⁵ Classical magnetoresistance results in positive magnetoresistance due to the fact that the applied magnetic field causes the electrons to attempt to go around periodic cyclotron orbits. The magnitude of classical magnetoresistance is on the order of $\mu^2 B^2$. Using a typical value for the mobility, $\mu \approx 10^{-4}$ cm²/V s, we estimate $\Delta R/R \approx 10^{-20}$ at $B \approx 10$ mT for classical magnetoresistance. The classical magnetoresistance is, therefore, much too small to explain OMAR at similar fields. In hopping magnetoresistance, an applied magnetic field shrinks the electron wave function and this reduces the overlap between hopping sites leading to an increase in resistance of the system resulting in a positive magnetoresistance effect. The size of this effect is only appreciable if the magnetic length λ is comparable to the hopping distance. In our case, λ ($=\sqrt{\hbar/eB}$, where \hbar and e have their usual meaning) is around 200 nm at 10 mT, which is much bigger than the hopping distance, which we estimate to be ≈ 10 nm at most. At low temperatures in disordered systems, corrections to the transport due to e-e interaction become important. This is mainly due to the fact that carriers interact often when they diffuse slowly. It can be shown that the e-e interaction is modified in the presence of a magnetic field; however, this occurs only if the thermal energy, kT , is less than or comparable to the Zeeman energy, $\Delta E = g\mu_B B$, where g is the g factor and μ_B is the Bohr magneton. In organics, $g \approx 2$ and therefore, $\Delta E \approx 1$ μ eV at a field of 10 mT, and therefore is much smaller than kT in our experiments. Therefore, this mechanism also fails to explain OMAR. Weak localization (WL) due to quantum corrections to the Drude-like transport is another mechanism for magnetoresistance. This mechanism is very well known from the study of diffusive transport in metals and semiconductors.⁴⁵⁻⁴⁷ It is based on backscattering processes due to constructive quantum interference. When a magnetic field is applied to the system, the quantum interference is destroyed by the magnetic field if the phase delay due to the enclosed magnetic flux exceeds the coherence length. Therefore, the resistivity is decreased (negative magnetoresistance effect). In WL theory, it is assumed that the spin-orbit coupling is weak. Strong spin-orbit coupling

would cause weak antilocalization (WAL), leading to a positive magnetoresistance effect due to destructive quantum interference.

Mechanisms (1) to (3) lead to positive magnetoresistance, whereas OMAR can also be negative. This implies that the observed magnetoresistance should not be due to either (1), (2), or (3). Interestingly, we note that the observed OMAR traces closely resemble magnetoresistance traces due to weak localization (WL, negative magnetoresistance) and weak antilocalization (WAL, positive magnetoresistance). An analysis of our data using WL theory,¹⁴ however, produces several surprising results that cast some doubts on this interpretation. For example, the weak temperature dependence of the effect is contrary to most if not all of the literature on WL and WAL in inorganic conductors. Furthermore, in WL theory, the width of the magnetoresistance cones is inversely proportional to the phase-breaking length, which in turn is intimately related to the mobility. We, however, observe equal magnetoresistance cone width in materials with largely different mobilities.

Frankevich and coworkers^{48,49} have shown that lifetimes of pairs of paramagnetic species (such as electrons and holes), which may be in singlet and triplet states, are very sensitive to external magnetic fields within the range of the hyperfine interaction. We note, however, that a recent experiment failed to observe this effect.³⁸ In general, models involving pairs of electrons and holes appear promising since typical magnetic dipole fields between pairs of electrons and holes can be expected to be on the order of 10 mT. However, it is not quite clear how the pairing mechanism should occur in hole-only devices, such as the Au-cathode-polyfluorene devices we studied, although spin-dependent bipolaron formation is a possibility. One might also expect that this mechanism should depend strongly on the carrier density, whereas OMAR is only weakly dependent on current density. In particular, intersystem crossing between singlet and triplet electron-hole pairs resulting from hyperfine interaction has been employed to explain the magnetic field effect on the electroluminescence in organic devices.^{15,18} In this model, the external magnetic field results in Zeeman splitting. If the Zeeman splitting exceeds the hyperfine interaction strength (this typically occurs at $B \approx 1$ mT), then mixing between singlets and the two extremal Zeeman levels of the triplets is no longer possible; therefore, the intersystem crossing rate is reduced. However, our observation that the width of the OMAR traces is unchanged in Pt-containing PPE compared to those in PPE, implies that this model cannot account for OMAR. This is because, as we have shown (see Fig. 10), the heavy Pt atom leads to an intersystem crossing rate that is very much stronger than that due to hyperfine interaction. Therefore, a much larger magnetic field should be required to prevent mixing between singlet and triplet levels.

Therefore, it appears that a novel explanation for the observed magnetoresistance effect needs to be found. This could lead to a better understanding of the transport processes in organic semiconductors. Follow-up experiments performed on current-in-plane devices and in devices using crystalline or oriented organic semiconductors will likely provide further clues to the origin of the OMAR effect.

V. CONCLUSION

In summary, we studied a recently discovered magnetoresistance effect in several different π -conjugated polymer and small molecular thin film devices. In polyfluorene devices at room temperature, we found that the magnitude of the effect is $\approx 10\%$ at fields on the order of 10 mT. The effect can be either positive or negative, depending on operating conditions. The effect is independent of the sign and direction of the magnetic field and is only weakly temperature dependent. Our experiments show that OMAR is a bulk effect related to the majority carrier (here hole) current. In PEDOT/polyfluorene/Ca devices, the OMAR effect can be described phenomenologically by a parallel translation of the $I-V$ curve to lower voltages as the magnetic field is applied. We also studied RR-P3HT and RRa-P3OT π -conjugated polymers to observe the effect of order and/or disorder, and therefore varying mobility, on OMAR. We found that the magnitude of the OMAR effect in the RRa-P3OT devices were consistently greater than that of the RR-P3HT devices. Therefore, low disorder and/or large mobility is not a necessary prerequisite for large OMAR response.

We also studied PPE and Pt-containing PPE polymers to check for a possible interrelation between spin-orbit coupling and the OMAR effect as a first step toward deciding whether OMAR is an orbital or spin effect. We found that spin-orbit coupling has apparently little effect on OMAR. This result excludes mechanisms based on processes that both involve the electron spin and that occur at time scales greater than 1 ns. In particular, processes involving intersystem crossing in excitons are excluded.

We also extended our study to small molecular devices. We observed a large OMAR effect in Alq₃ devices that is similar in size to that in the polyfluorene devices. As in polymers, the effect is independent of the sign and direction of the magnetic field, is only weakly temperature dependent, and is found to be related to the majority carrier current (here electrons). Since the current-voltage characteristics of the Alq₃ devices are typical of space-charge limited current, this implies that OMAR is not related to a magnetic field effect on the carrier injection. Similar to polyfluorene, in PEDOT/Alq₃/Ca devices, the OMAR effect can be described phenomenologically by a parallel translation of the $I-V$ curve to lower voltages as the magnetic field is applied. We found that the shift in voltage is quite insensitive to the temperature and that it increases proportionally with the device thickness.

Strikingly, we found that the functional dependence of the OMAR effect on B was very similar in all devices we studied. We showed that the set of empirical laws, $\Delta R/R \propto [B/(B+B_0)]^2$ and $\Delta R/R \propto B^2/(B^2+B_0^2)$ fits the experimental data well over almost three orders of magnitude in magnetic field in devices with weakly saturated and fully saturated behavior, respectively. However, close to the regions in parameter space where a transition from negative to positive OMAR occurs, these functions fail to fit the data and a more general expression must be found. The universality may point to the involvement of nuclear spin.

To the best of our knowledge, OMAR is not adequately described by any of the magnetoresistance mechanisms

known to date. Therefore, it may be related to the peculiar mode of charge transport in organic semiconductors, a field that still relatively little is known about. If one could find an explanation for this effect, this may lead to a breakthrough in the scientific understanding of organic semiconductors.

ACKNOWLEDGMENTS

We acknowledge fruitful and inspiring discussions with Professor M. E. Flatté and Professor Z. V. Vardeny. This work was supported by NSF Grant No. ECS 04-23911.

*Corresponding author. Electronic address: markus-wohlgenannt@uiowa.edu

- ¹R. H. Friend, R. W. Gymer, A. B. Holmes, J. H. Burroughes, R. N. Marks, C. Taliani, D. D. C. Bradley, D. A. D. Santos, J. L. Brédas, M. Löglund *et al.*, *Nature* (London) **397**, 121 (1999).
- ²S. R. Forrest, *Nature* (London) **428**, 911 (2004).
- ³C. J. Brabec, N. S. Sariciftci, and J. C. Hummelen, *Adv. Funct. Mater.* **11**, 15 (2001).
- ⁴S. R. F. Peter Peumans and Soichi Uchida, *Nature* (London) **425**, 158 (2003).
- ⁵M. Granström, K. Petritsch, A. C. Arias, A. Lux, M. R. Anderson, and R. H. Friend, *Nature* (London) **395**, 257 (1998).
- ⁶C. D. Dimitrakopoulos and P. R. L. Malenfant, *Adv. Mater.* (Weinheim, Ger.) **14**, 99 (2002).
- ⁷D. J. Gundlach, Y. Y. Lin, and T. N. Jackson, *IEEE Electron Device Lett.* **18**, 87 (1997).
- ⁸M. Shtein, J. Mapel, J. B. Benziger, and S. R. Forrest, *Appl. Phys. Lett.* **81**, 268 (2002).
- ⁹M. Wohlgenannt, K. Tandon, S. Mazumdar, S. Ramasesha, and Z. V. Vardeny, *Nature* (London) **409**, 494 (2001).
- ¹⁰V. Dediu, M. Murgia, F. C. Matalotta, C. Taliani, and S. Barbanera, *Solid State Commun.* **122**, 181 (2002).
- ¹¹Z. H. Xiong, D. Wu, Z. V. Vardeny, and J. Shi, *Nature* (London) **427**, 821 (2004).
- ¹²T. L. Francis, O. Mermer, G. Veeraraghavan, and M. Wohlgenannt, *New J. Phys.* **6**, 185 (2004).
- ¹³O. Mermer, G. Veeraraghavan, T. Francis, and M. Wohlgenannt, *Solid State Commun.* **134**, 631 (2005).
- ¹⁴O. Mermer, G. Veeraraghavan, T. L. Francis, and M. Wohlgenannt, *Weak Localization and Antilocalization in Polymer Sandwich Devices*, cond-mat/0312204 (unpublished).
- ¹⁵J. Kalinowski, M. Cocchi, D. Virgili, P. Di Marco, and V. Fattori, *Chem. Phys. Lett.* **380**, 710 (2003).
- ¹⁶J. Kalinowski, M. Cocchi, D. Virgili, V. Fattori, and P. Di Marco, *Phys. Rev. B* **70**, 205303 (2004).
- ¹⁷A. H. Davis and K. Bussmann, *J. Vac. Sci. Technol. A* **22**, 1885 (2004).
- ¹⁸Y. Yoshida, A. Fujii, M. Ozaki, K. Yoshino, and E. L. Frankevich, *Mol. Cryst. Liq. Cryst.* **426**, 17 (2005).
- ¹⁹G. Salis, S. F. Alvarado, M. Tschudy, T. Brunswiler, and R. Allenspach, *Phys. Rev. B* **70**, 085203 (2004).
- ²⁰J. Wilkinson, A. H. Davis, K. Bussmann, and J. P. Long, *Appl. Phys. Lett.* **86**, 111109 (2005).
- ²¹M. S. Khan, M. R. A. Al-Mandhary, M. K. Al-Suti, P. R. Raithby, B. Ahrens, L. Male, R. H. Friend, A. Kohler, and J. Wilson, *J. Chem. Soc. Dalton Trans.* **1**, 65 (2003).
- ²²J. S. Wilson, A. Köhler, R. H. Friend, M. K. Al-Suti, M. R. A. Al-Mandhary, M. S. Khan, and P. R. Raithby, *J. Chem. Phys.* **113**, 7627 (2000).
- ²³M. Redecker, D. D. C. Bradley, M. Inbasekaran, and E. P. Woo, *Appl. Phys. Lett.* **73**, 1565 (1998).
- ²⁴H. Bässler, *Polym. Adv. Technol.* **9**, 402 (1998).
- ²⁵A. H. Davis and K. Bussmann, *J. Appl. Phys.* **93**, 7358 (2003).
- ²⁶P. Stamenov and J. M. D. Coey, *J. Magn. Magn. Mater.* **290**, 279 (2005).
- ²⁷H. Sirringhaus, N. Tessler, and R. H. Friend, *Science* **280**, 1741 (1998).
- ²⁸H. Sirringhaus, P. J. Brown, R. H. Friend, M. M. Nielsen, K. Bechgaard, B. M. W. Langeveld-Voss, A. J. H. Spiering, R. A. J. Janssen, E. W. Meijer, P. Herwig *et al.*, *Nature* (London) **401**, 685 (1999).
- ²⁹R. Österbacka, C. P. An, X. M. Jiang, and Z. V. Vardeny, *Science* **287**, 839 (2000).
- ³⁰X. M. Jiang, R. Österbacka, O. Korovyanko, C. P. An, B. Horowitz, R. A. J. Janssen, and Z. V. Vardeny, *Adv. Funct. Mater.* **12**, 587 (2002).
- ³¹The mobilities cited here were measured in planar transistors in the relatively high-carrier density, low-electric field regime (see Ref. 50). Measuring carrier mobilities directly in sandwich devices has remained a challenge, and time-of-flight measurements can usually only be performed on very thick sandwich devices (Ref. 23) making the applicability to thin film devices again uncertain. Therefore, we cannot provide exact mobility values for our RR-P3HT and RRA-P3OT thin film devices, but it is reasonable to expect that RR-P3HT will show much higher mobilities.
- ³²J. S. Wilson, A. S. Dhoot, A. J. A. B. Seeley, M. S. Kahn, A. Köhler, and R. H. Friend, *Nature* (London) **413**, 828 (2001).
- ³³C. Yang, Z. V. Vardeny, A. Köhler, M. Wohlgenannt, M. K. Al-Suti, and M. S. Khan, *Phys. Rev. B* **70**, 241202(R) (2004).
- ³⁴Unfortunately, the photoluminescence spectrum of the organic PPE is much broader than that of the platinum-containing polymer and it is therefore possible, in principle, that a weak phosphorescence band is hidden under the stronger, broad fluorescence emission. However, from the works on many organic polymers, it is very well established that phosphorescence does not occur in continuous wave photoluminescence measurements.
- ³⁵S. V. Frolov, M. Liess, P. A. Lane, W. Gellermann, Z. V. Vardeny, M. Ozaki, and K. Yoshino, *Phys. Rev. Lett.* **78**, 4285 (1997).
- ³⁶H. F. Wittmann, R. H. Friend, and J. Lewis, *J. Chem. Phys.* **101**, 2693 (1994).
- ³⁷J. S. Wilson, N. Chawdhury, M. R. A. Al-Mandhary, M. Younus, M. S. Khan, P. R. Raithby, A. Kohler, and R. H. Friend, *J. Am. Chem. Soc.* **123**, 9412 (2001).
- ³⁸M. Reufer, M. J. Walter, P. G. Lagoudakis, B. Hummel, J. S. Kolb, H. G. Roskos, U. Scherf, and J. M. Lupton, *Nat. Mater.* **4**, 340 (2005).
- ³⁹The onset voltage in the Pt-PPE devices is roughly ten times higher than those in PPE devices. This discrepancy can, at least in part, be explained by the fact that our PPE devices were much

- thinner (this was necessary because of the low solubility of PPE in the casting solvent; no reliable layer thickness could be obtained from profilometer measurements) than the Pt-PPE ones.
- ⁴⁰R. G. Kepler, P. M. Beeson, S. J. Jacobs, R. A. Anderson, M. B. Sinclair, V. S. Valencia, and P. A. Cahill, *Appl. Phys. Lett.* **66**, 3618 (1995).
- ⁴¹L. S. Hung and C. H. Chen, *Mater. Sci. Eng., R.* **39**, 143 (2002).
- ⁴²J. M. Ziman, *Theory of Solids*, 2nd ed. (Cambridge University Press, Cambridge, 1972), Chap. 7, p. 250.
- ⁴³A. L. Efros and B. I. Shklovskii, *Electronic Properties of Doped Semiconductors* (Springer-Verlag, New York, 1984).
- ⁴⁴R. Menon, *Organic Photovoltaics* (Springer Verlag, New York, 2003), Chap. 3, pp. 91–117.
- ⁴⁵G. Bergmann, *Phys. Rep.* **107**, 1 (1984).
- ⁴⁶S. J. Papadakis, E. P. De Poortere, H. C. Manoharan, J. B. Yau, M. Shayegan, and S. A. Lyon, *Phys. Rev. B* **65**, 245312 (2002).
- ⁴⁷D. M. Zumbühl, J. B. Miller, C. M. Marcus, K. Campman, and A. C. Gossard, *Phys. Rev. Lett.* **89**, 276803 (2002).
- ⁴⁸E. L. Frankevich, A. A. Lymarev, I. Sokolik, F. E. Karasz, S. Blumstengel, R. Baughman, and H. H. Horhold, *Phys. Rev. B* **46**, 9320 (1992).
- ⁴⁹A. L. Buchachenko and E. L. Frankevich, *Chemical Generation and Reception of Radio- and Microwaves* (Wiley VCH, New York, 1994).
- ⁵⁰W. F. Pasveer, J. Cottaar, C. Tanase, R. Coehoorn, P. A. Bobbert, P. W. M. Blom, D. M. de Leeuw, and M. A. J. Michels, *Phys. Rev. Lett.* **94**, 206601 (2005).